Formation of hydroxyapatite on titanium implants *in vivo* precedes bone-formation during healing

Per Malmberg[a)]
Department of Chemistry and Chemical Engineering, Chalmers University of Technology, 412 96 Gothenburg, Sweden

Narmin Bigdeli
Department of Clinical Chemistry and Transfusion Medicine, Institute of Biomedicine, University of Gothenburg, 405 30 Gothenburg, Sweden

Jens Jensen
Department of Physics, Chemistry and Biology (IFM), Thin Film Physics, Linköping University, 581 83 Linköping, Sweden

Håkan Nygren
Department of Medical Chemistry and Cell Biology, Institute of Biomedicine, Sahlgrenska Academy at the University of Gothenburg, POB 440, 405 30 Gothenburg, Sweden

The bone material interface has been an area of intense study over many decades, where studies of the healing process ranging from simple mineral deposition *in vitro* to actual healing *in vivo* have given important clues to the importance of calcium minerals in the bone/implant interface. Here, the authors use a combination of *in vitro* cell culture methods and *in vivo* implantation to study how the role of the spontaneously formed hydroxyapatite layer on Ti-implants for the *in vivo*-healing into the bone tissue of rat tibia. Initial experiments were made in reduced systems by incubation of TiO_2 in cell culture medium and analysis by time of flight secondary ion mass spectrometry (ToF-SIMS) and energy-dispersive x-ray spectroscopy followed by subsequent exposure of human embryological stem cells analyzed by von Kossa staining and environmental scanning electron microsopy. *In vivo* studies of the bone–material interface was analyzed by ToF-SIMS depth profiling using both C_{60}^+ ions as well as a gas cluster ion source beam, Ar_{1500}^+ as sputter source. The low ion yield of the Ar_{1500}^+ for inorganics allowed the inorganic/organic interface of the implant to be studied avoiding the erosion of the inorganic materials caused by the conventional C_{60}^+ beam. © 2017 Author(s). All article content, except where otherwise noted, is licensed under a Creative Commons Attribution (CC BY) license (http://creativecommons.org/licenses/by/4.0/). https://doi.org/10.1116/1.4993986

I. INTRODUCTION

The bone–material interface of metal implants can be metaphorically described as an archaeological excavation site, where studies can deliver important clues to the mechanism of bone healing at material surfaces. Consequently, the bone-titanium implant border has remained an object of continuous study during four decades.[1–15] However, studies of the established material/bone interface cannot give definite answers to the time-dependence of the subprocesses of bone formation. The only possible way to obtain this information is to make time-lapse studies of bone healing at implants. The simplest system for such studies is to follow the mineral deposition onto titanium oxide from simulated body fluids,[16] or to analyze the adsorption of proteins and cells from blood onto titanium.[17] More complex studies can be made by analyzing bone healing at implants after various time periods of healing.[13]

Recently, we found that hydroxyapatite (HA) is formed spontaneously during incubation of Ti-implants with cell culture medium or blood.[18] The apatite formed was low crystalline carbonated hydroxyapatite as detected by x-ray photoelectron spectroscopy after incubation with cell culture medium [Dulbecco's modified Eagle's Medium (DMEM)] or low $CaCO_3$, as detected as CaO^+ by Time of flight secondary ion mass spectrometry (ToF-SIMS) after incubation in whole blood, suggesting that blood decreased the rate of HA-formation.[18] The HA layer on titanium is generally thought of as being formed by passive precipitation, but recent data on recovered implants show that Ti-surface is coated with Ca, indicating a binding between Ti and Ca as an early event in the healing process.[19]

The aim of the present study was to elucidate the role of the spontaneously formed HA layer on Ti-implants for the *in vivo*-healing into the bone tissue of rat tibia. The bone–material interface was analyzed by depth profiling using ToF-SIMS with both C_{60}^+ ions as well as a gas cluster ion source beam (GCIB) using Ar_{1500}^+. Experiments were also made in a reduced systems, incubation of TiO_2 in cell culture medium, analyzed by ToF-SIMS and energy-dispersive x-ray spectroscopy (EDX), and subsequent exposure of human embryological stem cells (hESCs) analyzed by von Kossa

[a)]Electronic mail: malmper@chalmers.se

staining of hydroxyapatite and environmental scanning electron microsopy (ESEM).

II. EXPERIMENT

A. Sample preparation

Commercial granules of TiO_2 (>99.9% pure, product 204757, lot MKBH6783V, Sigma-Aldrich, Stockholm, Sweden) were incubated in cell culture medium (DMEM, Gibco, Grand Island, NY. Product No. 11995-065) at 37 °C in humidified atmosphere for 24 h, rinsed in saline and distilled water, and dry sterilized at 160 °C for 2 h. The grain size was determined to 2 μm by light microscopy of a water suspension. Sterilized dental implants were used as received from Elos Medical AB (Timmersdala, Sweden) and were implanted into rats as described in Sec. II G.

B. Human mesenchymal stem cell culture

The human embryonic stem cell (hESC) lines used in this study were SA167MFG-hESC and AS034.1MFG-hESC at passage 12 and 44, respectively, derived and characterized in a previous study.[20] Cell culture was performed at the Department of Clinical Chemistry and Transfusion Medicine, Institute of Biomedicine, University of Gothenburg. Note that the stem cells used adhere to plastic surfaces and can be cultured in polystyrene dishes.

C. Expansion of hESCs

In this study hESCs were expanded and differentiated toward the osteogenic lineage directly onto tissue culture plastic without any supportive coating. In brief, cells were expanded in conditioned hES medium as described earlier containing 80% KnockOut^{TM} DMEM (Gibco-BRL/Invitrogen, Gaithersburg, MD), 20% KnockOut serum replacement (Gibco-BRL/Invitrogen), 2 mM L-glutamine (Gibco-BRL/Invitrogen), 0.1 mM β-mercaptoethanol (Gibco-BRL/Invitrogen), and 1% nonessential amino acids (Gibco-BRL/Invitrogen) on Primaria® dishes (Falcon, surface modified polystyrene nonpyrogenic; Becton Dickinson, Franklin Lakes) and were incubated in a humidified atmosphere at 37 °C and 5% CO_2 (Heraeus BBD6220). The SA167MFG-hESC and AS034.1MFG-hESC were passaged every 4–6 days, and the medium was changed every second day.

D. Exposure of stem cells to TiO_2 preincubated with DMEM

Undifferentiated hESCs were cultured on regular tissue culture plastic without predifferentiation stages such as embryoid body formation.

Cell exposure was performed by adding the HA-coated TiO_2 in concentrations of 5 or 0.5 mg/ml into the culture medium for 24 h.

E. Fixation and Von Kossa staining

Mineral production was studied using von Kossa staining performed by washing the cells in phosphate-buffered saline followed by fixation in glutaraldehyde solution (25% in H_2O Sigma-Aldrich diluted 1:10) for 2 h. A solution of $AgNO_3$ (2% w/v: Sigma-Aldrich) was added, and the plates were kept in dark for 10 min. The plates were then rinsed three times with distilled H_2O before being exposed to bright light for 15 min. After washing with distilled H_2O, samples were quickly dehydrated adding 100% EtOH prior to microscopic inspection for mineralization as described earlier.[21] Cells, fixed with glutaraldehyde and dehydrated in ethanol, were also analyzed by ESEM under low vacuum conditions.

F. Cell viability

hESCs were seeded onto a 24 well plate at density of 10 000 cells/well. Cells were incubated in growth medium with or without the presence of metal oxides for 24 h to allow for attachment. The attached cells were considered viable and floating cells nonviable.

G. Animal surgery

All animal work was approved by the Gothenburg animal experiment ethical committee. The surgery was performed as described in a previous study,[22] shortly as follows. Male Sprague Dawley rats 200 g (Charles River, Holland) were used. The animals were anesthetized with Isofluran (Baxter Medical CO, Kista, Sweden). A hole was drilled (d = 1 mm) in the tibial facies lateralis. Sterile dental Ti-implants (Elos Medtech, Timmersdala, Sweden) were implanted intramedullary. The surface chemistry was analyzed by EDX and found to be C 5.6%, O 13.2%, and Ti 94.5%. The animals were kept at the Experimental Biomedicine facility and were fed commercial pellets and water *ad libitum*. The animals were harvested after 24 or 72 h or 5 weeks by separating the heart from the main arteries, and the tibia bones were dissected. Four animals (eight implants) were used for ToF-SIMS analysis, and four animals were used for the EDX analysis.

H. Environmental scanning electron microscopy and EDX

The rat tibiae were immersed into absolute ethanol on dry ice. The bone tissue was substituted with alcohol for one week at −80 °C, warmed to room temperature, and cut with a diamond saw, using absolute ethanol as lubricating liquid and rinsed carefully in absolute ethanol. The samples were left to dry at room temperature. An FEI Quanta 200 FEG ESEM operating at an accelerating voltage of 20 kV was used for imaging and chemical analysis. All images were acquired in the backscattered electron imaging mode at a pressure of 1 Torr in the low vacuum region in order to avoid charging effects. Energy dispersive x-ray (EDX) data was recorded using an Oxford EDX detector and spectra were evaluated with the INCA software. Results were expressed as mass % of all detected elements or atom % for calculation of Ca/P ratio.

I. ToF-SIMS

ToF-SIMS analysis was performed with a TOF.SIMS 5 instrument (ION-TOF GmbH, Münster, Germany) using a

Bi_3^+ cluster ion gun as the primary ion source. Multiple (n = 5) regions ranging from 100×100 to 500×500 μm were analyzed using a pulsed primary ion beam (Bi_3^+, 0.34 pA at 25 keV) with a focus of approximately 2 μm and a mass resolution of M/ΔM = 5000 fwhm at m/z 500. All spectra were acquired and processed with the SURFACE LAB software (version 6.4, ION-TOF GmbH, Münster, Germany), and the ion intensities used for calculations were normalized to the total ion dose of each measurement. Depth profile analysis was performed using the pulsed Bi_3^+ gun (0.4 pA) while sputtering was carried out with a 10 keV C_{60}^+ beam with a current of 0.6 nA. The maximum ion dose density of Bi_3^+ was kept at 2×10^{11} ions cm^{-2} and therefore below that of the static limit, i.e., 1×10^{13} ions cm^{-2}, to make sure that the experiment was ended before the primary ion beam had considerably damaged the surface of the sample. The ion dose for C_{60}^+ ranged from 4×10^{14} to 6×10^{14} ions cm^{-2}. Low energy electrons were used for charge compensation during analysis. Profiles were also obtained using an argon gas cluster ion beam (GCIB) source, using 20 keV Ar_{1500} ions at a current of 0.364 nA. The ion dose for Ar_{1500} ranged from 4×10^{14} to 7×10^{14} ions cm^{-2}.

III. RESULTS AND DISCUSSION

The chemical composition of the samples was analyzed by EDX and ToF-SIMS before (data not shown) and after incubation in DMEM. The EDX data from the analysis of untreated TiO_2 showed (mass %): C 23.3, O 41, and Ti 35.1. After incubation in DMEM (n = 3), the sample showed (mass %): Ti 64.48 $\pm$ 8.80, Ca 0.63 $\pm$ 0.19, P 0.26 $\pm$ 0.15, O 29.79 $\pm$ 9.77, and C 3.83 $\pm$ 0.57. The Ca/P ratio (at. %) was 1.8.

Characterization of the TiO_2 samples, control and preincubated in DMEM by ToF-SIMS, is shown in Fig. 1. The control showed clear signals from Ti^+ and TiO^+ (range not shown) but no HA related peaks as can be seen in Fig. 1(a). ToF-SIMS was however able to detect several ion species from HA such as $Ca_2PO_4^+$, $Ca_3PO_5^+$, and Ca_5PO_7 on the DMEM incubated sample as indicated in the spectrum in Fig. 1(b).

The HA-coated TiO_2 powder was then added to hESC cultures. The cells proliferated during their exposure to the TiO_2 grains. The loss of adhering cells was less than 10% of the cell layer surface. Images of the exposed cell cultures are shown in Fig. 2. Figure 2(a) shows a low magnification ESEM image of the cell layer and polystyrene surfaces without cells. On the polystyrene surfaces, single TiO_2 grains or small aggregates of grains are seen. On the cell layer, the TiO_2 grains have been taken up by the cells, as judged by light microscopy and excreted into extracellular areas between the cells. These aggregates are shown at higher magnification in Fig. 2(b). Figure 2(c) shows an untreated cell culture control. Figure 2(d) shows von Kossa stain image of the cultured hESCs exposed to DMEM-preincubated TiO_2. The cell layer contains silver precipitate indicating the presence of mineral. As shown by Bonewald *et al.*,[23] the von Kossa staining is not specific for HA, but can also stain "dystrophic mineralization of unknown
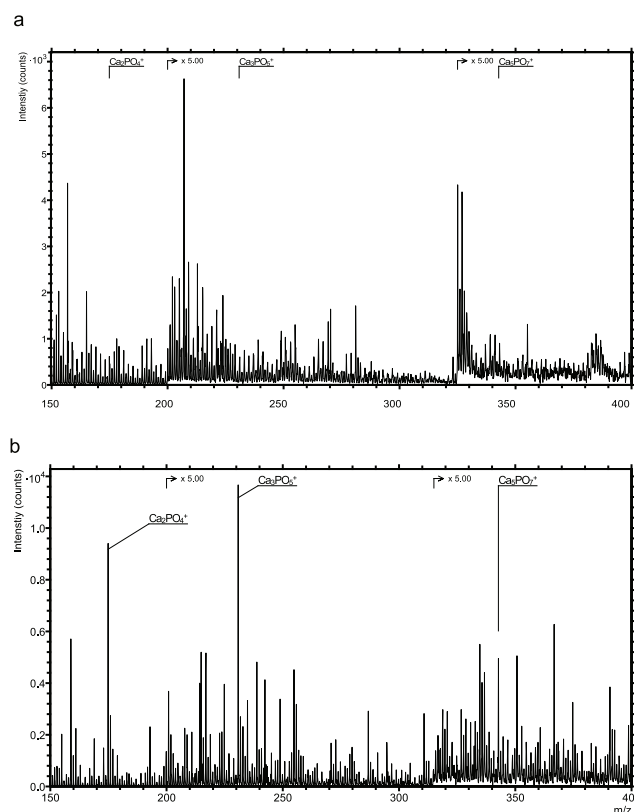

FIG. 1. (a) ToF-SIMS spectrum of control TiO_2 powder. No hydroxyapatite related ions can be detected. Total fluence 1.9×10^{12}. (b) ToF-SIMS spectrum of TiO_2 powder incubated in media analyzed with Bi_3^+ ions. Ions from hydroxyapatite $Ca_2PO_4^+$, $Ca_3PO_5^+$, and $Ca_5PO_7^+$ are indicated. Total fluence was 1.18×10^{12}.

chemical composition." Since the added TiO_2 grains are coated with low levels of HA, they may be stained by the von Kossa. The aggregated TiO_2 particles shown in Figs. 2(a) and 2(b) are also seen by light microscopy [Fig. 2(e)]. The aggregate pattern of TiO_2 grains in this image may be compared to the von Kossa stained culture [Fig. 2(d)]. From this experiment, we conclude that the cells, apparently, add mineral to the aggregates during the process of uptake and excretion.

Ti-implants were operated into rat tibia and allowed to heal for 24–72 h. The tissue layer formed during the first 3 days of healing was analyzed with depth profiling ToF-SIMS as shown in Figs. 3(a)–3(c). Figures 3(a) and 3(b) show data generated by conventional C60$^+$ sputtering and Fig. 3(c) data generated by sputter using a gas cluster ion source using Ar_{1500}^+. The C60$^+$ based profiles show a similar behavior with an initial layer consisting of cells and organic matter, represented by the phosphatidylcholine headgroup, $C_5H_{15}PNO_4^+$, stemming from phosphatidylcholine and phosphatidylethanolamine molecules, followed by a HA layer, represented by signals from P_2OH^+ and $Ca_2PO_4^+$. The CaO^+ signal, likely stemming from $CaCO_3$, peaks at approximately 0.8×10^{14} ions/cm^2 and is detected immediately before the titanium signal. The signal eventually decays before the Ti^+ reaches its maximum. Very little difference can be found between the 48 and 72 h samples with regards to the organic and HA layers while the CaO layer
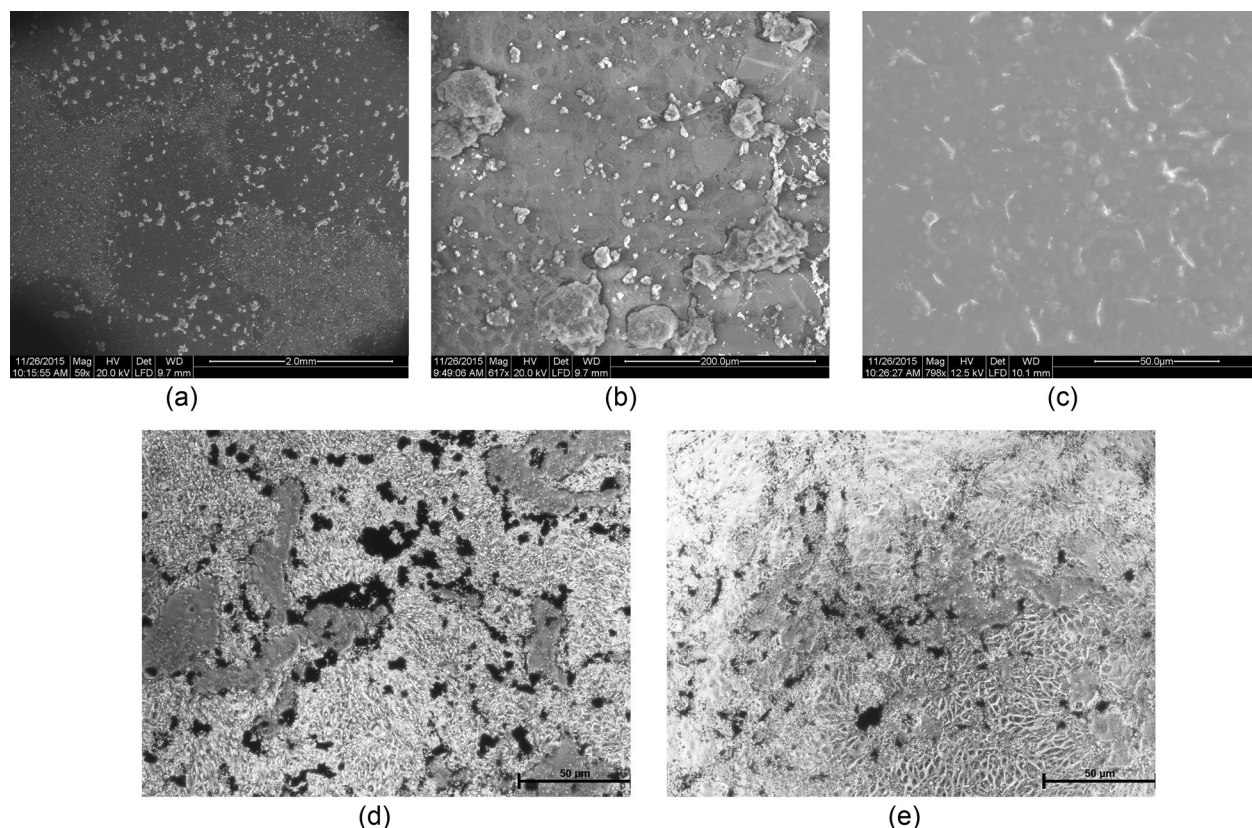
FIG. 2. Human embryonic stem cells grown for 24 h with or without the presence of 0.5 mg/ml of TiO_2 grains, with a diameter of 2 μm, preincubated in DMEM. After 24 h, the cells were fixed with 2.5% glutaraldehyde. (a) ESEM image of the surface of the culture dish showing cell-covered areas with large aggregates of TiO_2 grains and polystyrene areas with single grains or small clusters of TiO_2 grains. Bar = 2 mm. (b) ESEM image of the cell layer of cultured hESCs with large aggregates of TiO_2 grains in extracellular spaces, single grains or small clusters of TiO_2 grains. Bar = 200 μm. (c) ESEM image of the cell layer of hESCs cultured in DMEM for 24 h and fixed in glutaraldehyde. Bar = 50 μm. (d) Von Kossa staining of the cell layer of hESCs cultured in the presence of TiO_2 grains. The Von Kossa-positive staining shows large aggregates of mineral in extracellular spaces. (e) Light microscopy of the cell layer of hESCs cultured in the presence of TiO_2 grains.

possible appears to be thicker for the 48 h implanted surface. Depth profiling using argon GCIB produces a somewhat different result as seen in Fig. 3(c), where the argon is unable to erode the CaO away fully and CaO reached maximum at 3 $\times 10^{14}$ ions/cm^2 but never fully sputters away as for C_{60}^+. The Ar_{1500}^+ beam is clearly not as efficient as C_{60}^+ in sputtering the inorganic CaO layer. Ar clusters are known to be very efficient in sputter removing organic layers without any damage, but sputter inorganic material very slowly or not at all depending on cluster size and energy.[24–26]

The elemental composition of the cut bone was C 27.3; N 4.06; O 35.94; Mg 0.44; P 11.8; and Ca 22.94. The elemental composition of the bone in contact with the implant was C 28.31; N 4.43; O 28.3; Mg 0.28; P 11.3; and Ca 26.75. However, the Ca levels are higher than the corresponding values of untreated bone.[27] The implant related bone thus seems to be identical to the compact cortical bone after 5 weeks of healing and the compact bone is affected by the healing in of the implant, which is in accord with previous findings during healing of MgO into bone.[27] The 2D morphology of the implant-related bone shows an archipelague structure of the bone, interdigitated with areas of bone marrow.

The time period of bone healing, 48–72 h, used in the present study was chosen based on previous results from studies on the time dependence of bone healing at titanium implants.[13,28–30] Callus bone appears in the wound after 96 h, apparently originating and extending from the endosteum and periosteum. The presented results show that the titanium implant is coated with a stratified layer containing CaO^+ on the titanium surface, HA in an intermediate stratum, and phosphatidylcholine from cell membranes were found in an outer stratum, as seen in Fig. 3. This layering has been confirmed by previous studies, showing crystals of HA beneath the cells.[5,8] The inner stratum of Ca on the Ti surface has been described previously after analysis of the bone-implant interface of healed-in implants by atom probe tomography.[19] This analytical method can only detect basic elements and does not provide molecular information. The result of the present study, made by analysis with ToF-SIMS, suggests that the inner layer contains CaO, probably representing a Calcium mineral such as $CaCO_3$ or $Ca(HCO_3)_2$ transformed to CaO by heat-generated sublimation of CO_2 in the ion beam. The formation of a CaO-layer on Ti-implants after 1 week of healing, as analyzed by ToF-SIMS, has been reported previously.[31] After this time of healing, the bone
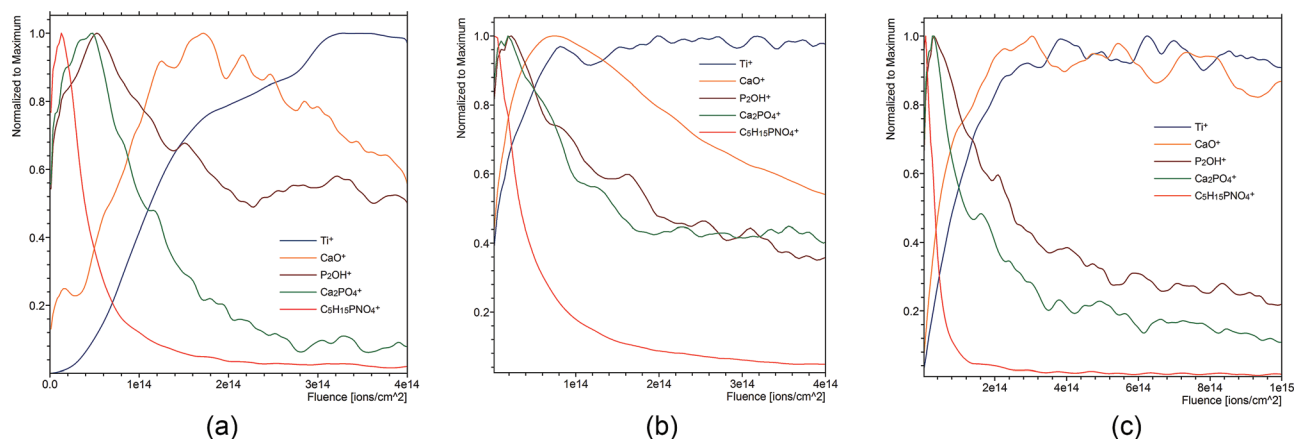
FIG. 3. (a) Depth profiling of an *in vivo* titanium implant after 48 h of healing using C_{60}^+. Depth profile analysis was performed using the pulsed Bi_3^+ gun to analyze an area of 156×156 μm while sputtering at 400×400 μm was carried out with a C_{60}^+ beam with a current of 0.6 nA. Ti is shown in blue, CaO^+ in orange, P_2OH^+ in brown, $Ca_2PO_4^+$ in green, and $C_5H_{15}PNO_4^+$ in red. Data are shown as normalized to maximum. Total fluence was 4×10^{14} ions/cm² for the C_{60}^+ ions. (b) Depth profiling of an *in vivo* titanium implant after 72 h of healing using C_{60}^+. Depth profile analysis was performed using the pulsed Bi_3^+ gun to analyze an area of 216×216 μm while sputtering at 300×300 μm was carried out with a C_{60}^+ beam with a current of 0.6 nA. Ti is shown in blue, CaO^+ in orange, P_2OH^+ in brown, Ca_2PO4^+ in green, and $C_5H_{15}PNO_4^+$ in red. Data are shown as normalized to maximum. Total fluence was 4.0×10^{14} ions/cm² for the C_{60}^+ ions. (c) Depth profiling of an *in vivo* titanium implant after 72 h days of healing using argon GCIB. Depth profile analysis was performed using the pulsed Bi^{3+} gun to analyze an area of 70×70 μm while sputtering at 500×500 μm was carried out with a Ar_{1500}^+ beam with a current of 1.3 nA. Ti^+ is shown in blue, CaO^+ in orange, P_2OH^+ in brown, $Ca_2PO_4^+$ in green, and $C_5H_{15}PNO_4^+$ in red. Data are shown as normalized to maximum. Total fluence shown 1×10^{15} ions/cm² for the argon ions.

marrow cavity is filled with callus bone and it is not certain whether bone-mineral or Ca-mineral is detected. Also, the ion gun used in the previous study did not allow for detection of the HA-derived fragments[32] as could be seen here, and that are now routinely observed using cluster ion ToF-SIMS.[33]

Here, we also see a clear difference in sputter ability between the conventional C_{60}^+ source and the GCIB argon source. Even though the information about the different layers are similar between the different sources, the argon GCIB quickly erodes the organic material from the implant while the inorganic CaO layer remains virtually unaffected on the Ti surface as can be seen in Fig. 3(c). This is in contrast to C60+ that slowly erodes also the CaO layer from the Ti surface. This is to be expected since GCIB sources are well known or their high sputter yield for organic materials compared with inorganic materials making them highly suitable for probing inorganic/organic implant surfaces.[26,34]

The results of several previous studies indicates the existence of an organic stratum at the surface of a titanium implant.[3,5,8] This finding can still be a valid one and there is no contradiction between the data presented here and previously published findings. As shown in Fig. 4, the titanium surface is coated with approximately equally sized areas of bone and bone marrow after 5 weeks of healing. It is undisputable that a titanium surface in contact with blood is rapidly covered with plasma proteins and platelets,[17] while the CaO layer is formed at a lower rate,[18] which means that it forms by diffusion of Ca^{2+} through the pre-existing organic layer. The results of a previous study indicates that the formation of the HA-layer was slower in blood than in the cell culture medium, whereas the $CaCO_3$ layer was formed at equal rates in both liquids, which can be explained by

inhibitory binding of osteopontin to the HA-layer. Osteopontin is known to regulate the formation of HA,[35] and has been detected by immunocytochemistry at the bone-implant interface.[36] Osteopontin is not believed to affect the differentiation of stem cells.[37] Thus, it was important to perform the present study of the process of HA-coating of Ti-implants *in vivo*. The presented data indicate that HA is formed *in vivo* on top of a layer of $CaCO_3$. This can be seen in both the C_{60}^+ as well as $Argon_{1500}^+$ depth profiles where HA is a clearly separated layer just below the organic
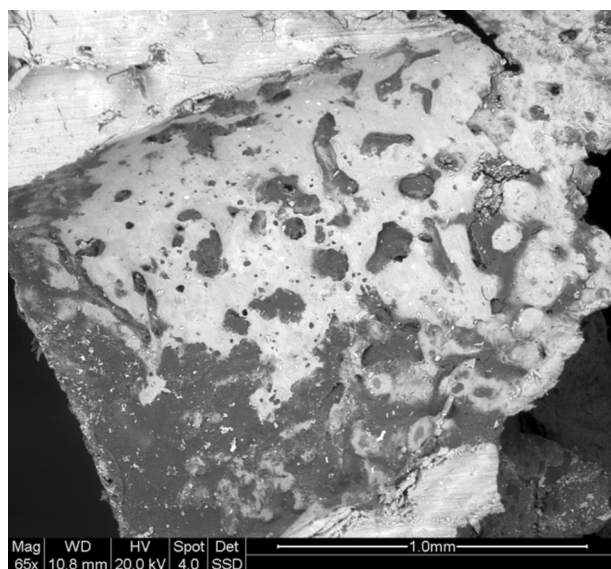

FIG. 4. Ti-implant-related bone after 5 weeks of healing. Compact bone, surrounding the implant has been cut with a diamond saw. Bone in contact with the implant (white areas) and soft tissue in contact with the implant (dark areas) are shown.

components from cells and membranes, and CaO^+ can be seen tightly connected to the Ti implant itself. Hence the implant is first coated by $CaCO_3$, then phosphate before the HA layer, which is then covered by cells and organic material. The argon GCIB shows the most accurate result here due to its low inorganic sputter yield hence allowing us to probe the still intact inorganic CaO/Ti interface.

The production of HA by stem cells exposed to HA-coated TiO_2, as can be seen in Fig. 2, can be regarded as a stress reaction and is not necessarily a sign of stem cell differentiation, since differentiation of embryonic stem cells to osteoblasts is expected to take 7 days rather than 24 h.[38] However, stem cells can be a significant source of HA at the bone-implant interface during bone healing, and HA itself seems to promote the differentiation of stem cells.[39]

IV. SUMMARY AND CONCLUSIONS

We have demonstrated the advantage of using argon GCIB for analyzing *in vivo* implants where now the organic/inorganic interface can be probed much more accurately. The results suggest that the established view of bone healing, that bone progenitor cells react with the TiO_2 surface, must be reevaluated since the formation of hydroxyapatite on the implant surface occurs more rapidly than the induction of bone formation. The actual sequence of events is that recruited stem cells are reacting to their contact with hydroxyapatite at the Ti-surface. This insight is important for a proper understanding of how implants heal into bone.

ACKNOWLEDGMENT

[1]J. Acero, J. Calderon, J. I. Salmeron, J. J. Verdaguer, C. Concejo, and M. L. Somacarrera, J. Cranio-Maxillofac. Surg. **27**, 117 (1999).

[2]T. Albrektsson, P.-I. Brånemark, H.-A. Hansson, and J. Lindström, Acta Orthop. Scand. **52**, 155 (1981).

[3]Y. Ayukawa, F. Takeshita, T. Inoue, M. Yoshinari, M. Shimono, T. Suetsugu, and T. Tanaka, J. Biomed. Mater. Res. **41**, 111 (1998).

[4]J. E. Davies, Biomaterials **28**, 5058 (2007).

[5]J. E. Davies, B. Lowenberg, and A. Shiga, J. Biomed. Mater. Res. **24**, 1289 (1990).

[6]M. Degidi, A. Piattelli, J. A. Shibli, V. Perrotti, and G. Iezzi, Int. J. Oral Maxillofac. Implants **24**, 896 (2009).

[7]G. Iezzi *et al.*, Implant Dent. **25**, 380 (2016).

[8]L. Linder, T. Albrektsson, P. I. Branemark, H. A. Hansson, B. Ivarsson, U. Jonsson, and I. Lundstrom, Acta Orthop. Scand. **54**, 45 (1983).

[9]T. Masuda, G. E. Salvi, S. Offenbacher, D. A. Felton, and L. F. Cooper, Int. J. Oral Maxillofac. Implants **12**, 472 (1997).

[10]T. A. Mian, M. C. Van Putten, Jr., D. C. Kramer, R. F. Jacob, and A. L. Boyer, Int. J. Radiat. Oncol., Biol., Phys. **13**, 1943 (1987).

[11]L. Sennerby, L. E. Ericson, P. Thomsen, U. Lekholm, and P. Astrand, Clin. Oral Implants Res. **2**, 103 (1991).

[12]S. Vandergugten, M. A. Cornelis, P. Mahy, and C. Nyssen-Behets, Eur. J. Orthod. **37**, 325 (2015).

[13]C. Eriksson, K. Ohlson, K. Richter, N. Billerdahl, M. Johansson, and H. Nygren, J. Biomed. Mater. Res. A **83**, 1062 (2007).

[14]K. Grandfield, A. Palmquist, and H. Engqvist, Philos. Trans. A Math. Phys. Eng. Sci. **370**, 1337 (2012).

[15]G. Sundell, C. Dahlin, M. Andersson, and M. Thuvander, Acta Biomater. **48**, 445 (2017).

[16]T. Kokubo and S. Yamaguchi, Acta Biomater. **44**, 16 (2016).

[17]C. Eriksson, H. Nygren, and K. Ohlson, Biomaterials **24**, 4759 (2004).

[18]H. Nygren, L. Ilver, and P. Malmberg, J. Funct. Biomater. **7**, 7 (2016).

[19]J. Karlsson, G. Sundell, M. Thuvander, and M. Andersson, Nano Lett. **14**, 4220 (2014).

[20]N. Bigdeli, M. Andersson, R. Strehl, K. Emanuelsson, E. Kilmare, J. Hyllner, and A. Lindahl, J. Biotechnol. **133**, 146 (2008).

[21]T. Tallheden, J. E. Dennis, D. P. Lennon, E. Sjogren-Jansson, A. I. Caplan, and A. Lindahl, J. Bone Joint Surg. Am. A **85**, 93 (2003).

[22]H. Nygren, M. Chaudhry, S. Gustafsson, G. Kjeller, P. Malmberg, and K. E. Johansson, J. Funct. Biomater. **5**, 158 (2014).

[23]L. F. Bonewald, S. E. Harris, J. Rosser, M. R. Dallas, S. L. Dallas, N. P. Camacho, B. Boyan, and A. Boskey, Calcif. Tissue Int. **72**, 537 (2003).

[24]C. M. Mahoney and G. Gillen, *Cluster Secondary Ion Mass Spectrometry* (Wiley, New York, 2013), pp. 1–11.

[25]K. Shen, D. Mao, B. J. Garrison, A. Wucher, and N. Winograd, Anal. Chem. **85**, 10565 (2013).

[26]K. Shen, A. Wucher, and N. Winograd, J. Phys. Chem. C **119**, 15316 (2015).

[27]H. Nygren, N. Bigdeli, L. Ilver, and P. Malmberg, Biointerphases **12**, 02C407 (2017).

[28]L. F. Cooper, J. Prosthet. Dent. **80**, 439 (1998).

[29]L. F. Cooper, T. Masuda, P. K. Yliheikkilä, and D. A. Felton, Int J. Oral Maxillofac. Implants **13**, 163 (1998).

[30]T. Masuda, P. K. Yliheikkilä, D. A. Felton, and L. F. Cooper, Int. J. Oral Maxillofac. Implants **13**, 17 (1998).

[31]C. Eriksson, K. Borner, H. Nygren, K. Ohlson, U. Bexell, N. Billerdahl, and M. Johansson, Appl. Surf. Sci. **252**, 6757 (2006).

[32]C. Eriksson, P. Malmberg, and H. Nygren, Rapid Commun. Mass Spectrom. **22**, 943 (2008).

[33]A. Henss, M. Rohnke, T. El Khassawna, P. Govindarajan, G. Schlewitz, C. Heiss, and J. Janek, J. R. Soc. Interface **10**, 20130332 (2013).

[34]P. J. Cumpson, J. F. Portoles, A. J. Barlow, N. Sano, and M. Birch, Surf. Interface Anal. **45**, 1859 (2013).

[35]G. K. Hunter, C. L. Kyle, and H. A. Goldberg, Biochem. J. **300**, 723 (1994).

[36]M. D. McKee and A. Nanci, Annals New York Acad. Sci. **760**, 177 (1995).

[37]E. Holm, J. S. Gleberzon, Y. Liao, E. S. Sorensen, F. Beier, G. K. Hunter, and H. A. Goldberg, Biochem. J. **464**, 355 (2014).

[38]H. Nagai *et al.*, J. Mater. Sci.: Mater. Med. **26**, 99 (2015).

[39]X. R. Chen, J. Bai, S. J. Yuan, C. X. Yu, J. Huang, T. L. Zhang, and K. Wang, Chem.-Biol. Interact. **238**, 111 (2015).